

N 9 3 - 2 9 6 3 2

INDUCED ACTIVATION STUDY OF LDEF

B. A. Harmon, G. J. Fishman, and T. A. Parnell
ES62 NASA/Marshall Space Flight Center
Huntsville, AL 35812
Phone: 205/544-4924, Fax: 205/544-7754

C. E. Laird

Department of Physics, Eastern Kentucky University
Richmond, KY 40475
Phone: 606/622-1526, Fax: 606/622-1020

SUMMARY

Analysis of the induced radioactivity of the Long Duration Exposure Facility (LDEF) is continuing with extraction of specific activities for various spacecraft materials. Data and results of activation measurements from eight facilities are being collected for interpretation at Eastern Kentucky University and NASA/Marshall Space Flight Center.

The major activation mechanism in LDEF components is the proton flux in the South Atlantic Anomaly (SAA). This flux is highly anisotropic, and could be sampled by taking advantage of the gravity-gradient stabilization of the LDEF. The directionally-dependent activation due to these protons has clearly been observed in the data from aluminum experiment tray clamps (reaction product ^{22}Na), steel trunnions (reaction product ^{54}Mn and others) and is also indicated by the presence of a variety of nuclides in other materials. A secondary production mechanism, thermal neutron capture, has been observed in cobalt, indium, and tantalum, which are known to have large capture cross sections. Experiments containing samples of these metals and significant amounts of thermalizing low atomic number (Z) material showed clear evidence of enhanced activation of ^{60}Co , $^{114\text{m}}\text{In}$ and ^{182}Ta . Other mechanisms which activate spacecraft material that are not as easily separable from SAA proton activation, such as galactic proton bombardment and secondary production by fast neutrons, are being investigated by comparison to radiation environmental calculations (Armstrong and Colborn, 1991, 1993). Deviations from one-dimensional radiation models indicate that these mechanisms are more important at greater shielding depths.

In this paper, we review the current status of the induced radioactivity measurements as of mid-year 1992. We present specific activities for a number of materials which show SAA effects and thermal neutron capture. We also examine the results for consistency by combining data from the participating institutions.

INTRODUCTION

In the First Post-Retrieval LDEF Symposium (Harmon, et al., 1991a), we discussed some of the major constituents of the space radiation environment which contributed to the activation of LDEF, and detailed a few of the measurements which illustrated their effects. A number of results were also presented by Smith and Hurley (1991), Moss and Reedy, and Winn from measurements made as a part of the cooperative effort to study the induced radioactivity of LDEF (Harmon, et al., 1991a,b). Further work by Smith and Hurley (1993), Reeves, et al., and Reedy, et al., can be found in these conference proceedings. Eight laboratories with low-level background detectors for gamma ray counting participated in a large scale study of LDEF radioactivity: Westinghouse/Savannah River Site (SRS), Pacific Northwest Laboratory/Battelle Memorial Institute (PNL), the Tennessee Valley Authority Western Area Radiological Laboratory (TVA), Lawrence Livermore National Laboratory (LLNL), Lawrence Berkeley Laboratory (LBL), Los Alamos National Laboratory (LANL), NASA/Johnson Space Center (JSC) and NASA/Marshall

Space Flight Center (MSFC). All received samples of spacecraft material following retrieval of LDEF in January 1990. Our efforts over the past year have been in collecting the results of induced radioactivity measurements from these laboratories, evaluating these results for consistency and quality, and extracting information about the radiation environment. Eventually all measurements will become part of a LDEF radiation database following evaluation. NASA/Marshall Space Flight Center and Eastern Kentucky University are primarily involved in a collaborative effort to produce this database and support a long-term archive. (Details can be found in the contribution by Laird, et al.) In this report, we attempt to bring together results from different laboratories and examine them in a coherent fashion. The data presented are, unavoidably, in various stages of completeness. While the measurement techniques are straightforward, extracting specific activities can be difficult for unusual sample geometries or samples which significantly attenuate the gamma rays of interest. In some cases, for identical geometries, different methods have been used to obtain the detector efficiency. (The efficiency relates the observed gamma-ray counting rate to the activity of the sample.) This can induce systematic uncertainties in the measured activity which can be larger than the statistical counting errors. We find systematic differences as large as 30% in some of the results reported here. We present these results with the caution that comparisons between measurements at different laboratories be regarded as preliminary until the evaluation is complete.

Materials obtained from LDEF in the months following retrieval are listed in Table I below. A detailed plan for analysis of these materials can be found in Harmon, et al., 1993. Further information and early results of the induced radioactivity investigations can be found in Harmon, et al., 1991b.

Aluminum	Experiment tray clamps and spacer plates, clamp assemblies, end support retainer plate, keel plate, scuff plate spacers, ballast covers, and end frame clamps
Titanium	Structural clips
Steel	End frame trunnions, tray clamp screws, and P0004/P0006 canister screws
Lead	Ballast plates
Other Samples	Vanadium, Nickel, Cobalt, Tantalum, and Indium (Exps. M0001, M0002, P0006, and A0114) Magnesium, Silver, Copper, Niobium, Molybdenum and Germanium (Exps. A0114 and A0171)

ALUMINUM

Many aluminum components (6061 alloy) at various shielding thicknesses were available from the spacecraft (see Table I). The most significant result from these was the mapping of the ^{22}Na activity (half-life 2.6 years, 511 and 1275 keV gamma rays) around the spacecraft using the experiment tray clamp plates (East, West, North and South directions) (Harmon, et al., 1991a,b). The activation was clearly peaked in the West direction, offset to the South, consistent with the expected angular distribution of the SAA proton flux (Watts, et al.). In order to obtain these results, about 50 clamp plates were counted at the Tennessee Valley Authority (TVA) Western

Area Radiological Laboratory. Several clamp plates have been counted at other laboratories to verify the extraction of the activities. In Table II, we present recent measurements from Winn (private comm.) at SRS and activities for the same clamp plates counted earlier by Frederick (private comm.) at TVA. All measurements presented have been decay-corrected to the date of LDEF return to Earth (January 20, 1990). Even though we are limited to only a common sample of six plates, comparison of these results shows that the trends are reasonably consistent between the two datasets. The computed differences between measurements also appear consistent with statistical error.

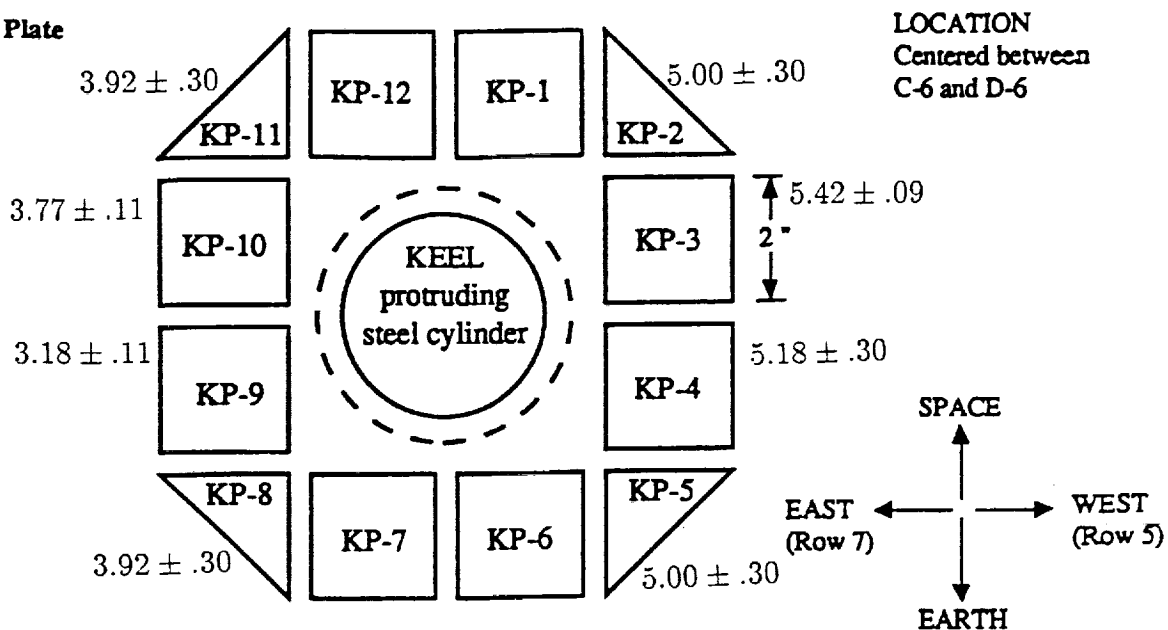
Sample ID	Activity (SRS) (dis/sec/kg)	Activity (TVA) (dis/sec/kg)	Difference (dis/sec/kg)
B7-5	4.61 ± .19	4.46 ± .38	-.15 ± .42
D7-2	5.17 ± .18	5.83 ± .38	+.66 ± .42
G6-4	5.34 ± .22	6.26 ± .81	+.92 ± .84
G6-10	3.55 ± .18	3.29 ± .56	-.26 ± .59
H6-4	4.80 ± .20	4.55 ± .64	-.25 ± .67
H9-12	4.63 ± .16	4.76 ± .81	+.13 ± .82

Winn obtains the efficiency for thin samples such as the clamp plates via a model where the efficiency is separable into two factors for the area and thickness of the sample. Point-like calibration sources and aluminum attenuator blanks are used to map out the areal and depth dependences of the efficiency over a range of gamma-ray energies. Using parameters derived from the calibration, the total peak efficiency is calculated by integrating the model expression. In addition, because the measurements were made with a high efficiency 90% germanium detector, a summing correction is also required to the peak efficiency for ²²Na. This is due to multiple emission of 511 keV (positron annihilation) and 1275 keV gamma radiation when ²²Na decays. The summing correction to the 1275 peak efficiency was measured to be 1.72 for the 90% detector (Winn, private comm.). Frederick at TVA (private comm.) used a mixed gamma source of the same area as the clamp plate (2" x 5") which eliminates the need for an area integral. The efficiency is then computed as a direct average of measurements of the calibration source placed in the front and back of the clamp plate. The lower efficiency germanium detectors at TVA (15%-30%) have a negligible summing correction for ²²Na. Mathematically, the only difference between the methods used by SRS and TVA is the treatment of the self-attenuation of the sample as an exponential in relating the "front" and "back" efficiency of the sample by Winn. This is critical for thick samples (see trunnion section studies below), but does not yield significantly different results from direct averaging for the thin clamp plates.

The experiment tray spacer plates, which were mounted beneath the clamp plates, also showed detectable ²²Na, mostly on the West side of the LDEF. These results have not been systematically analyzed, but show activities of 2-3 dis/sec/kg.

The keel plate (row 6, North side of LDEF) and the end support retainer plate (Earth end of LDEF) were both cut into samples roughly of 2"x2" area and individually counted at different laboratories. A composite representation of the ²²Na activities from LBL (Smith and Hurley, 1991), LANL (Moss and Reedy), and SRS (Winn) measurements is shown in Fig. 1. The keel plate was exposed to the westerly-peaked SAA flux and shows a correspondingly higher activity

(a) Keel Plate



(b) End Support Retainer Plate

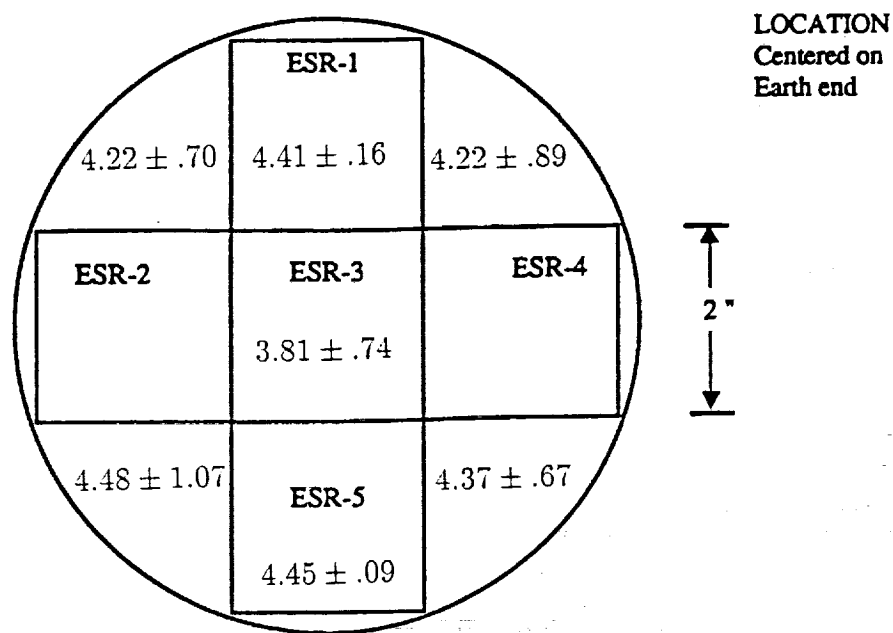


Figure 1. (a) Aluminum keel plate and (b) end support retainer plate showing the pattern in which samples were cut for activation analysis. ^{22}Na activities (dis/sec/kg) are shown for each sample. Activities for samples KP-1, 6, 7, and 12 and ESR-2 and 4 have not been reported.

in KP-2, 3, 4 and 5 (KP-2 and KP-5 were counted together) than KP-8, 9, 10, 11 (KP-8 and KP-11 were counted together). The retainer plate, which saw flux mainly from the Earth direction, has a much more uniform activation. The activity of the end support retainer plate should be compared to the earth end clamp plate data for G6-4 and G6-10 listed in Table II above.

The clamp assemblies, located behind the main (central) trunnion scuff plates, were the thickest samples of aluminum obtained from LDEF. These were large annular rings surrounding the main trunnions, which were cut and analyzed for directional and depth dependences, similar to the steel trunnions (see below). Some of the results for clamp assembly layers are given by Reeves and Frederick (private comm.); however, most of the measurements have not been reported. The scuff plate spacers and end frame clamps have also been counted; however, their geometry is too complex to extract specific activities easily. Both materials contained ^{22}Na and ^7Be activity. The ballast plate covers were rectangular plates mounted over the lead ballast on each end of LDEF. Some of the cover material was processed into normalizable 2"x2" squares and analyzed, but no activities have been reported.

TITANIUM

A number of titanium structural clips (6AL-4V alloy) were obtained from the internal frame of LDEF. The clips were mounted beneath the end intercostals, joining the intercostals to the longerons. Several groups Smith and Hurley (1991), Moss and Reedy, and Harmon report ^{46}Sc and ^{22}Na to be present in these samples. Obtaining specific activities are possible and appear to be in the range of 0.1-1 dis/sec/kg for ^{22}Na (Smith and Hurley, 1991) and about 0.5-1.5 dis/sec/kg for ^{46}Sc . The activation for ^{22}Na is considerably lower than that of the aluminum components, and is related to the heavier target (^{48}Ti , 73.7% natural abundance) and also the increased local shielding from the LDEF structure. The geometry of these samples (slanted parallelepiped cross section) will limit the accuracy of these measurements; nevertheless, these data are unique because of the atomic number Z being fairly well-removed from other analyzed materials ($Z=13$, 22 and 26 respectively for aluminum, titanium, and iron).

STEEL

^{54}Mn (half-life 312 days, 834 keV gamma ray) was expected to have the highest activity level in the steel trunnions (17-4PH alloy) based on the average energy of the trapped proton flux as well as the cross section for protons on iron (75% of 17-4PH). With an activity of 2-5 dis/sec/kg, it was possible to process the 20 in (50.8 cm) long by 3.25 in (8.26 cm) diameter cylinder into smaller cylindrical sections and concentric layers so that the ^{54}Mn activity could be mapped throughout the trunnion volume (Harmon, et al. 1991a,b). Directional and energy information about the activating particle fluxes could then be obtained. Figure 2 is a plot of the bulk ^{54}Mn activity in the two stainless steel trunnions from the Earth end of LDEF. The abscissa represents the distance along the trunnion axis measured from the end of the trunnion farthest from the spacecraft. Each point represents the average activity for one of the large cylindrical sections (3.25 in dia, from 0.5 to 1 in thickness). The space-exposed end of the "LH" trunnion was pointed West and offset to the North by the reported 8 degree yaw (Peters and Gregory), such that the axis of the trunnion was at an approximately 30 degree angle to the peak of the South Atlantic Anomaly proton flux angular distribution.

As indicated in Fig. 2, several counting groups have analyzed the large cylindrical sections. These have a large self-attenuation of 834 keV gamma rays (as much as 50%) which must be accurately assessed in order to extract a reliable specific activity. This becomes even more of a problem for ^{57}Co (122 keV) or ^{51}Cr (320 keV) activities, because of the rapid increase in attenuation for lower energy gamma rays. Winn has discussed in detail the required procedures for obtaining specific activities from these samples using point-like calibration sources. Frederick (private comm.), Lindstrom (private comm.), and Harmon have used a mixed gamma (planar)

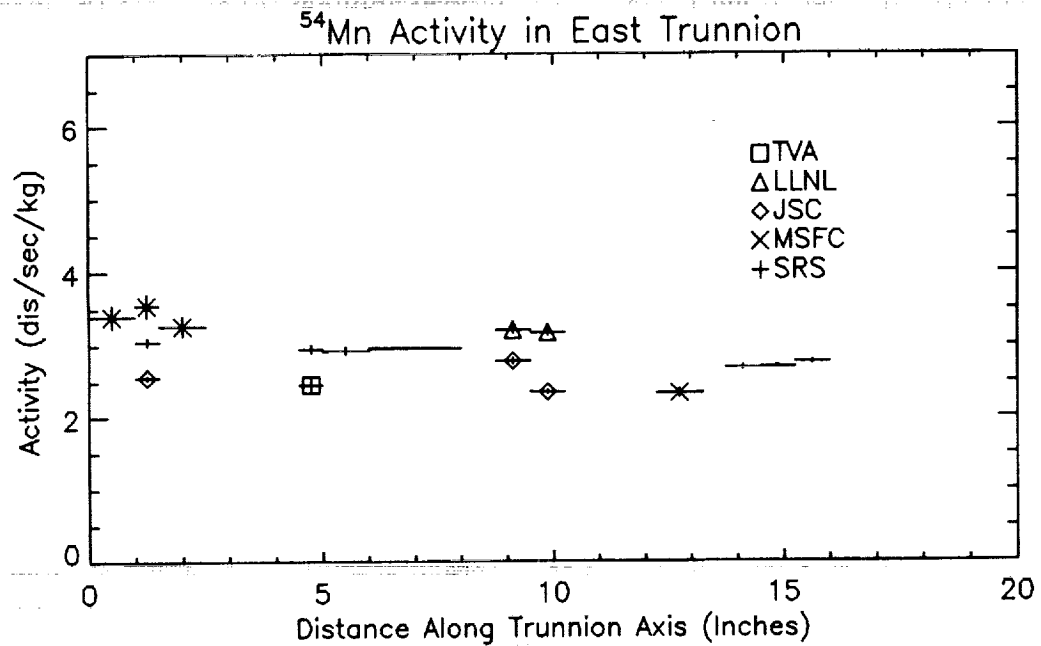
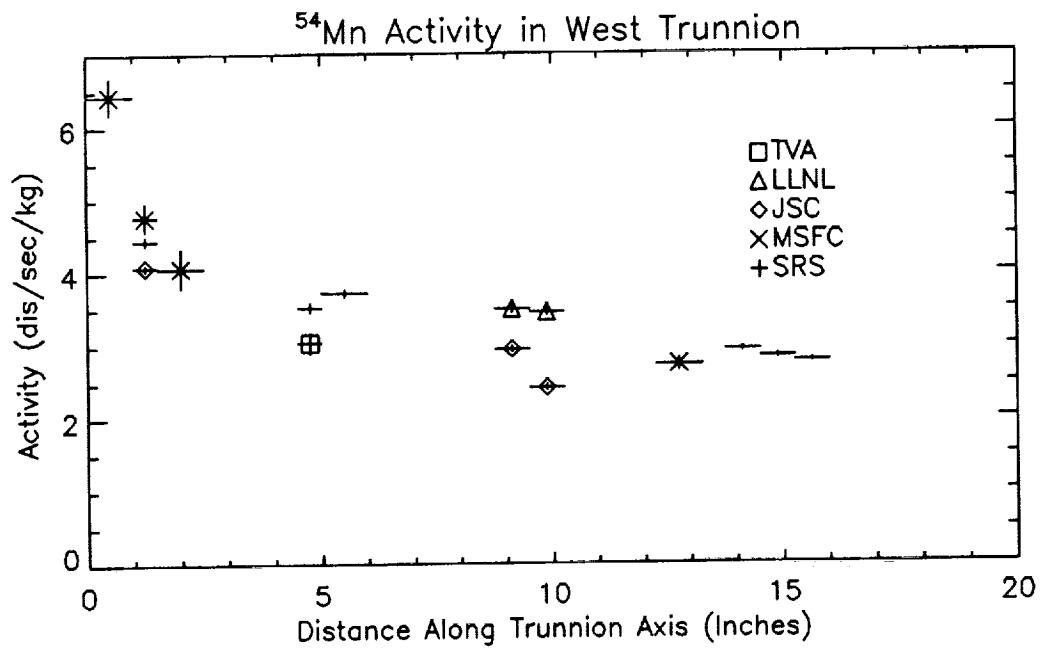


Figure 2. ^{54}Mn activities in the end frame steel trunnion as a function of distance along the trunnion center line. The origin of the horizontal axis represents the end of the trunnion farthest from the spacecraft.

grid source of the same diameter as the trunnion, which appears to give results comparable to the point source mapping technique. However, while the statistical error for several day counts of the large trunnion pieces is small as shown in Fig. 2, systematic differences in the activity at the 20-30% level are evidently present based on several measurements of the same sample (see activities measured at approximately 1, 5, 9 and 10 in in both East (RH) and West (LH) trunnions). The systematic differences also tend to be consistent between datasets. Both trunnions indicate a decreasing activity toward the spacecraft, with the SAA flux out of the West enhancing the activity considerably in the first two inches of the West trunnion. SAA protons are not energetic enough to penetrate the entire length of the trunnion and would not explain the more gradual decrease, which may be due to shielding from the spacecraft.

Three of the cylindrical sections from each of the two end trunnions were sliced into thin concentric layers about the trunnion axis, then quartered with a set of seven layers facing toward Earth, Space, North and South. The thinness and uniformity of the steel layer samples, coupled with the distribution of 2" x 2" mixed gamma standards to several of the counting laboratories, have made it much easier to extract activities from the layer samples than for the thick cylindrical sections discussed above. Results from each of the laboratories so far indicate reasonably consistent agreement with the trends and absolute magnitude of the activities as a function of direction and depth. Figure 3 shows the ^{54}Mn activity in trunnion layers from the LH (West) trunnion at a distance of approximately 7 inches from the end of the trunnion. These represent the most sensitive measurements to date of the steel layers. The observed differences in the North, South, Space and Earth directions are qualitatively similar to that in Harmon, et al., 1991b, where another layered section closer to the spaceward end of the trunnion was analyzed. The higher sensitivity measurements indicate a very significant difference in flux between North and South. The SAA exposure should produce an enhancement to the South (relative to North) due to the southwesterly peak of the proton flux. There is also a smaller Space-Earth asymmetry, which is at least partially attributable to shielding by the spacecraft on the space side of the trunnion (Armstrong and Colborn, 1991).

The only other steel components obtained from the LDEF were canister screws from experiments P0004 and P0006, and a large number of screws associated with the experiment tray clamps. These were generally too small to obtain sufficient statistics from counting of individual screws. Bulk counting by LLNL (Camp, private comm.) showed the presence of ^{54}Mn , ^{56}Co , ^{57}Co , ^{58}Co , ^{22}Na and ^7Be (surface deposition) with the $^{54}\text{Mn}/^{57}\text{Co}$ ratio being about 1.6-2.0 in the tray clamp screws, and a West/East ratio in the activities of 1.2-1.3. The $^{54}\text{Mn}/^{57}\text{Co}$ ratio appears to be quite different from the steel in the trunnions ($^{54}\text{Mn}/^{57}\text{Co} = 8-12$). The presence of significant amounts of ^{22}Na , which may be related to low mass impurities, was not expected, and is under investigation. Results for the P0004/P0006 screws have not been reported.

LEAD

Lead, taken from lead sheets used for ballast, was the highest atomic number ($Z=82$) material obtained for activation measurement. The lead ballast and associated aluminum cover plates were mounted on the end frame I-beams and were obtained several months following retrieval. Only ^{207}Bi at a very low activity has been reported by Smith and Hurley (1993) and Lindstrom (private comm.). No accurate activities have been obtained, but are estimated to be about 10^{-2} - 10^{-1} dis/sec/kg. Measured activities for both the aluminum and lead components are of interest due to the shielding effects from other parts of the spacecraft.

INTENTIONALLY-PLACED SAMPLES

Sets of vanadium, nickel, tantalum, indium, and cobalt metal samples, typically 2"x2" by 0.25" thick, were placed in four experiments (M0001, M0002, P0006 and A0114) on the LDEF. These constituted the original activation sub-experiment by Fishman (Harmon, et al., 1993)

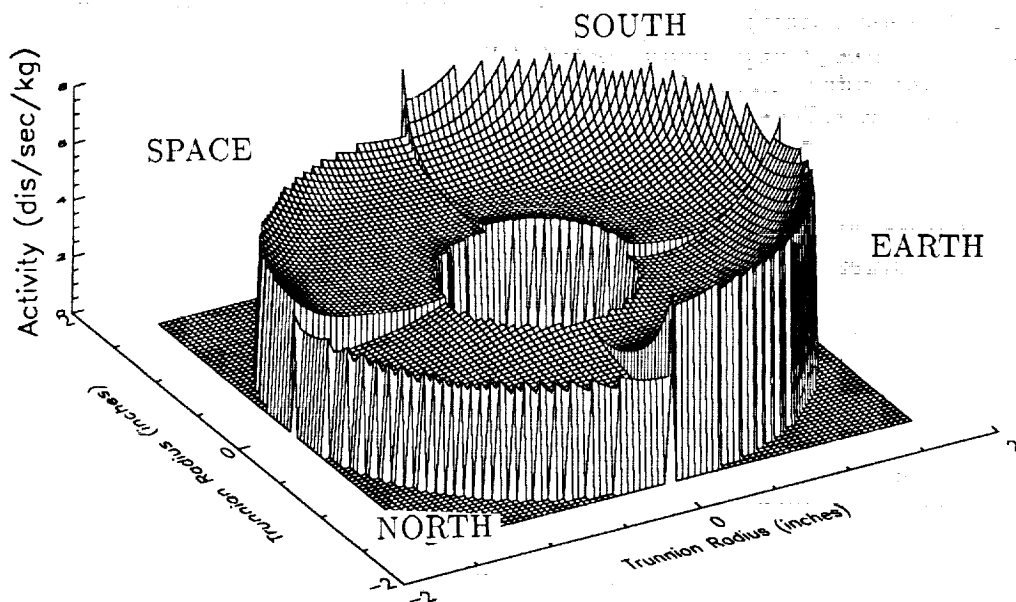
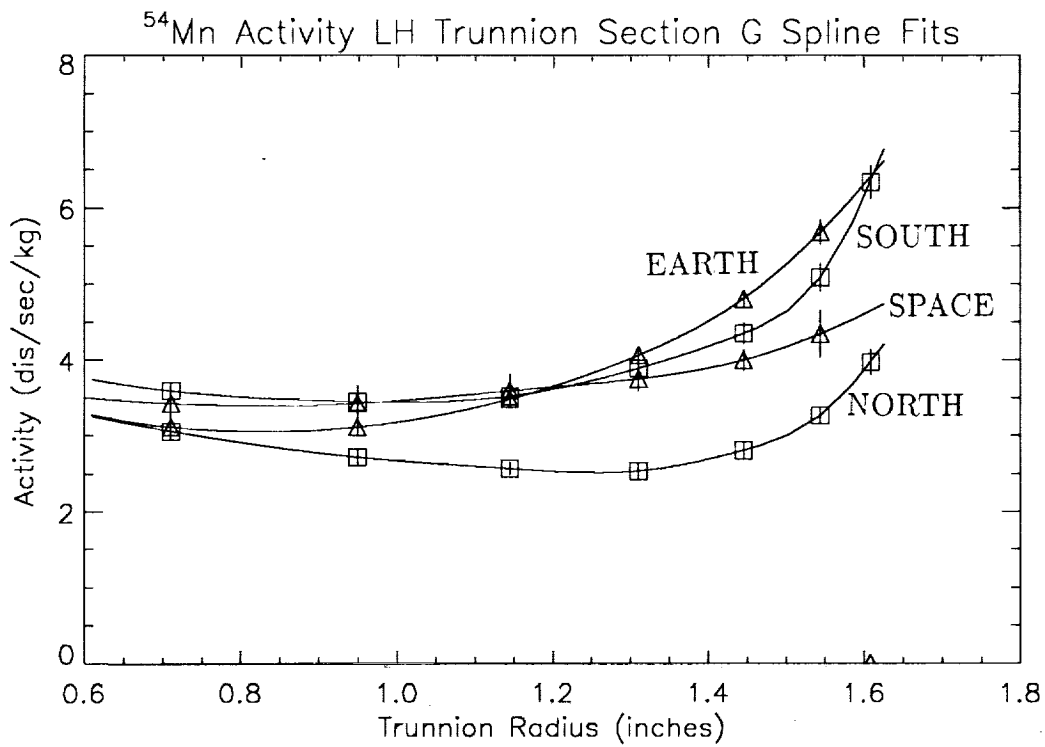


Figure 3. ^{54}Mn activity as a function of radius and direction for thin steel layers taken from the West (LH) trunnion. Top figure shows the activity profiles in the Earth, Space, North and South directions. Continuous curves represent a spline fit to the data. The spline fits were then used to create the bottom figure, which is an approximate two-dimensional representation of the activity throughout the cylindrical section. For clarity, no smoothing of the directional variation was performed.

for monitoring the on-orbit induced radioactivity. Many of these samples have been counted by different laboratories and provide a good basis for interlaboratory comparisons of absolute measurements. All of these materials, with the exception of nickel are monoisotopic or nearly so, which reduces the ambiguity of the reactions producing certain nuclides. Smith and Hurley (1991), Winn, Reeves, et al., and Camp (private comm.) have reported results for samples exchanged between laboratories. Table III gives a comparison of all activities for intentional samples which have been counted at more than one laboratory. Blanks indicate that no activity was detected. Recent measurements by Reeves, et al., of the G12 (M0002) cobalt with both an ultra low-level germanium and NaI coincidence system yields ^{60}Co activities of $1.01 \pm .10$ and $1.26 \pm .08$ dis/sec/kg, respectively. Generally the agreement is good for most nuclides, except for the ^{54}Mn and ^{57}Co in the G12 (M0002) cobalt, which is under investigation.

Table III. Comparison of Activities for LDEF Activation Foils					
G12 (M0002) Cobalt			G12 (M0002) Indium		
Nuclide	LLNL (dis/sec/kg)	LBL (dis/sec/kg)	Nuclide	LLNL (dis/sec/kg)	LBL (dis/sec/kg)
^{54}Mn	$3.38 \pm .14$	$2.31 \pm .05$	^{102}Rh	—	$.085 \pm .011$
^{56}Co	$0.82 \pm .14$	—	^{110m}Ag	—	$.085 \pm .011$
^{57}Co	$11.2 \pm .20$	$7.82 \pm .06$	^{113}Sn	$.80 \pm .14$	$.78 \pm .04$
^{58}Co	$4.30 \pm .73$	—	^{114m}In	—	$1.3 \pm .56$
^{60}Co	$0.97 \pm .08$	$0.85 \pm .03$	^{88}Zr	$.64 \pm .11$	—
G12 (M0002) Vanadium		F2 (P0006) Vanadium			
	SRS	LLNL		SRS	LBL
^{46}Sc	$.59 \pm .05$	$.59 \pm .05$	^{46}Sc	$.72 \pm .08$	$.64 \pm .04$

Most of the radionuclides listed in Table III are products expected from proton-induced reactions. However, tantalum, indium, and cobalt also have high thermal neutron capture cross sections. These foils are activated by very low energy thermal and epithermal ($\geq .02\text{eV}$) neutrons that are moderated by low Z material on the LDEF. Only a few experiments carried significant amounts of plastic or organic compounds which slow energetic neutrons (some are made as secondary products from the proton-induced reactions, others may be atmospheric albedo neutrons). Reeves, et al., report an enhanced ^{60}Co (neutron capture on ^{59}Co) activity in the M0001 experiment (Adams, et al.), which contained plastic cosmic ray track detectors, relative to ^{60}Co activities in the other experiments. Similarly, the ^{182}Ta (neutron capture on ^{181}Ta) is higher in the M0001 experiment and the P0004/6 experiments (Benton, et al., and Alston) which contained plastic detectors and organic materials. A comparison of the neutron capture activities in the three foils is shown in Fig. 4, which represents a composite of data from LBL (Smith and Hurley, 1993), PNL (Reeves, et al.), and JSC (Lindstrom, private comm.). Neglecting formation and decay rates, the trends appear consistent between experiments. The only exception is experiment M0001, which apparently showed a lower tantalum activation than cobalt or indium. The ^{182}Ta (115 day half-life) activity will decrease relative to ^{60}Co (5.27 year half-life) due to the decrease in proton flux at the lower altitudes encountered in the later part of the mission. The activity of ^{114m}In (49.5 day half-life, neutron capture on ^{113}In (4.3% natural abundance)) is somewhat

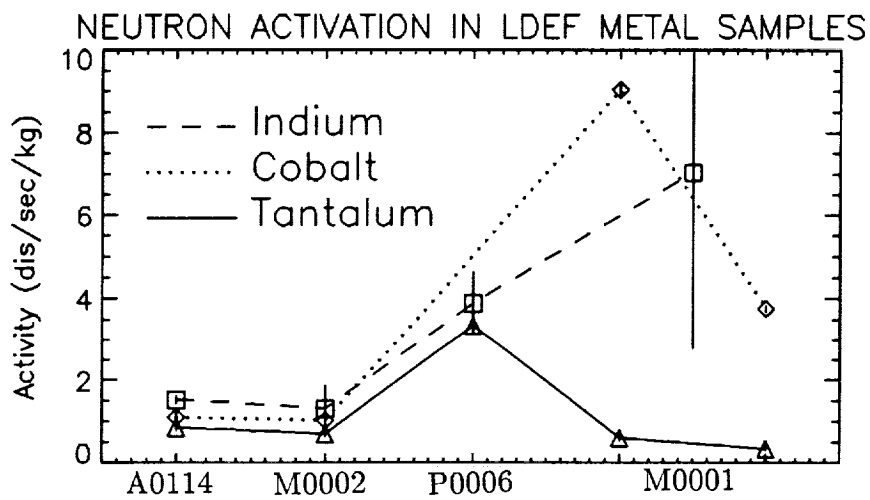


Figure 4. Neutron capture activities for indium, cobalt and tantalum metal samples from Exps. A0114, M0001, M0002 and P0006. Exp. M0001 had two samples of the same metal, one near the edge of the experiment tray and one near the center. (See text for further explanation.) Exp. P0006 did not contain a cobalt sample.

inconsistent with this picture, yet the indium could be a factor of 2-3 lower and still be within the large 1-sigma uncertainty. In addition, ^{114m}In includes a significant fraction of proton-induced activation from ^{115}In (95.7% abundance). The metal samples in Experiment M0001, which were delivered for integration in the standard 2"x2" geometry, had to be cut into two smaller pieces of approximately 2" x 3/4" for mounting on opposite sides of a subtray. The tantalum and cobalt were counted separately, and interestingly show a difference in activity between two sides of the tray. This is directly related to the amount of low Z material in proximity to the samples, which was greater on one side than the other. In the near future, it may be possible to deduce reasonably accurate local thermalized neutron fluxes from these measurements.

OTHER MATERIALS

A few small metal samples were obtained from other experiments (magnesium, silver, copper, niobium, molybdenum and germanium) several months after retrieval. Almost all had no detectable activity, at the 0.1-1 dis/sec/kg level or higher with the exceptions of magnesium (^{22}Na) and germanium (^{65}Zn). Olmez, et al., 1991, 1993, reported results for larger samples of copper and zirconium, which showed the presence of ^{58}Co and ^{88}Y , respectively, consistent with production by trapped SAA protons.

CONCLUSION

We have surveyed the overall status of the activation measurements performed on the LDEF spacecraft components. Although all samples have been counted, a significant fraction of the results have not been reported. Collection, analysis and evaluation of measurements are continuing. It is planned to complete these phases of the investigation by the end of 1993, and shift the effort toward developing a complete picture of the external radiation fluxes, secondary reactions and the shielding/geometric effects on the results. Complementary studies of LDEF dosimetric and activation data should sufficiently constrain calculations of the low earth orbit radiation environment and allow better prediction of radiation doses for future space missions.

REFERENCES

- Adams, J. H., et al.: Preliminary Results from the Heavy Ions in Space Experiment. First Post-Retrieval LDEF Symposium, NASA CP-3134, 1991, p. 377.
- Alston, J. A.: Seeds in Space Experiment. First Post-Retrieval LDEF Symposium, NASA CP-3134, 1991, p. 1625
- Armstrong, T. W. and B. L. Colborn: Ionizing Radiation Calculations and Comparisons with LDEF Data. First Post-Retrieval LDEF Symposium, NASA CP-3134, 1991, p. 347.
- Armstrong, T. W. and B. L. Colborn: Radiation Model Predictions and Validation Using LDEF Data. Second Post-Retrieval LDEF Symposium, NASA CP-3194, 1993.
- Benton, E. V., et al.: Radiation Exposure of LDEF: Initial Results. First Post-Retrieval LDEF Symposium, NASA CP-3134, p. 325.
- Harmon, B. A., et al.: Induced Radioactivity in LDEF Components. First Post-Retrieval LDEF Symposium, NASA CP-3134, 1991, p. 301.
- Harmon, B. A., G. J. Fishman, T. A. Parnell, E. V. Benton and A. L. Frank: LDEF Radiation Measurements: Preliminary Results. Nucl. Tracks and Rad. Meas. **20**, No. 1, 1991, p. 131.
- Harmon, B. A., G. J. Fishman, and T. A. Parnell: LDEF Induced Radioactivity Analysis Plan. NASA TM-103545, 1993.
- Laird, C. E., et al.: Collection, Analysis, and Archival of LDEF Activation Data. Second Post-Retrieval LDEF Symposium, NASA CP-3194, 1993.
- Moss, C. E. and R. C. Reedy: Measurement of Induced Radioactivity in Some LDEF Samples.

- First Post-Retrieval LDEF Symposium, NASA CP-3134, p. 271.
- Olmez, I., et al.: Charged Particle Activation Studies on the Surface of LDEF Spacecraft. First Post-Retrieval LDEF Symposium, NASA CP-3134, 1991, p. 255.
- Olmez, I., et al., Second Post-Retrieval LDEF Symposium, NASA CP-3194, 1993.
- Peters, P. N. and J. C. Gregory: Pinhole Cameras as Sensors for Atomic Oxygen in Orbit; Application to Attitude Determination of the LDEF. First Post-Retrieval LDEF Symposium, NASA CP-3134, 1991, p. 61.
- Reedy, R., et al.: Radioactivities Induced in Some LDEF Samples. Second Post-Retrieval LDEF Symposium, NASA CP-3194, 1993.
- Reeves, J., et al.: Sensitivity of LDEF Foil Analyses Using Ultra- Low Background Germanium vs. Large NaI(Tl) Multidimensional Spectrometers. Second Post-Retrieval LDEF Symposium, NASA CP-3194, 1993.
- Smith, A. R. and D. L. Hurley: Radioactivities of Long Duration Exposure Facility (LDEF) Materials: Baggage and Bonanzas. First Post-Retrieval LDEF Symposium, NASA CP-3134, 1991, p. 257.
- Smith, A. R. and D. L. Hurley: A Photon-Phreak Digs the LDEF Happening. Second Post-Retrieval LDEF Symposium, NASA CP-3194, 1993.
- Watts, J., et al.: Approximate Angular Distributions and Spectra for Geomagnetically-trapped Protons in Low-Earth Orbit. AIP Conf. Proc. 186, High Energy Radiation Background in Space, Ed. by A. C. Rester and J. I. Trombka (AIP, New York), 1989, p. 75.
- Winn, W. G.: Gamma-Ray Spectrometry of LDEF Samples at SRS. First Post-Retrieval LDEF Symposium, NASA CP-3134, 1991, p. 287.